CHALMERS
UNIVERSITY OF TECHNOLOGY

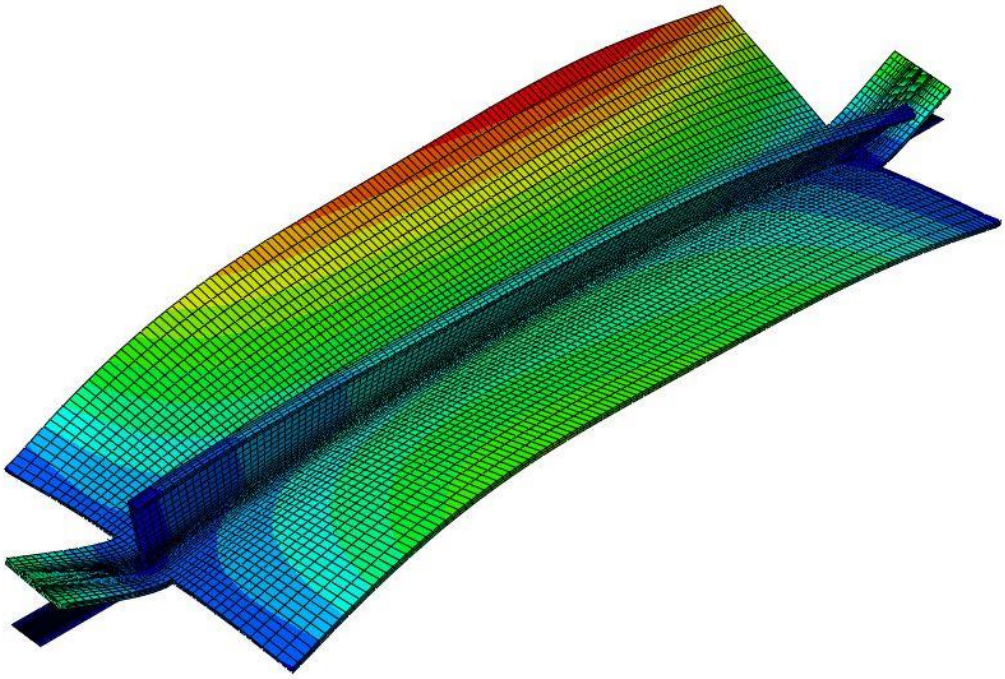

Deformations and Stresses in Welded Panels

Development and analysis of a simulation procedure for two-pass fillet welding of a stiffener to a plate

Project in Applied Mechanics, TME131

Thangam Boominathan
Aditya Pujari
Wilhelm Sjödin
Monika Stoyanova

Supervisors:
Shivaprasad Gurram
Lennart Josefson
Moyra McDill

DEPARTMENT OF MECHANICS AND MARITIME SCIENCES

CHALMERS UNIVERSITY OF TECHNOLOGY
Gothenburg, Sweden 2021

Deformations and stresses in welded panels

TME131 Project in Applied Mechanics 2021

Studentarbeten – Mekanik och maritima vetenskaper (M2) – Projektarbeten 2021:08

Department of Mechanics and Maritime Sciences
Chalmers University of Technology
SE-412 96 Gothenburg
Sweden
Telephone +46 (0)31-772 1000

Cover: Deformed mesh after two-pass fillet welding of a stiffener to a plate.

Preface

The work in the present report was carried out as a part of the course TME131 Project in Applied Mechanics, which is a mandatory course within the Applied Mechanics Masters programme at Chalmers. The course was carried out during the fourth period in the spring 2021.

The project was supervised by Prof. Lennart Josefson (Chalmers University of Technology), Prof. Em Moyra McDill (Carleton University) and Shivaprasad Gurram.

Abstract

This project is a part of the Masters programme Applied Mechanics at Chalmers and will also be a contribution to a benchmark exercise in a Specialist Committee, V.3 Material and Fabrication Technology for the International Ship and Offshore Structures Congress (ISSC) 2022 Conference. The goal of this project is to further develop and analyse an existing simulation procedure for two-pass fillet welding of a stiffener to a plate with the aim to find what simplifications that can be made in the modelling. The results from finite element simulations (FE-simulations) are then compared to analytical solutions and experimental data for validation.

The FE-simulations are carried out with the commercial FEA-software ABAQUS using forward-coupled thermal-mechanical FE-simulations with geometrical and material nonlinearities included. The analysis is first performed on a shorter plate (200 mm) to draw faster conclusions by saving computational time. Once the analysis for the shorter plate has been conducted, a longer plate (1000 mm) representing the benchmark geometry is analysed.

To verify that a simplified model of the heat input can be used, FE-simulations on the short plate are used to calculate the cooling time between 800˚C and 500˚C at a node on the weld. This data is then used to compare with analytical solutions for the cooling time in this interval, valid for the weld parameters specific to this benchmark project. By adapting the weld speed and maximum temperature of the weld, the optimal cooling time, and parameters for the heat input, are found. The simplified heat source model then gives the same behaviour as a real weld.

With the thermal simulation settings validated by analytical solutions, the results from the mechanical part of the FE-simulations are analysed for the short plate. Here different sequences of releasing mechanical boundary conditions are studied, and how they affect the residual deformations after the two-pass fillet welding. This is achieved in ABAQUS by changing simulation steps and compiling the deformation fields for different configurations. Furthermore, different methods for preventing rigid body motion (RBM) are analysed and their influence on the residual deformations. Mechanical contact between a table beneath the plate is modelled using Lagrange multipliers creating a hard contact. The effect of this contact modelling on the residual deformations is also investigated, whether it is necessary or not since a removal of contact conditions will reduce computational cost considerably. One conclusion that can be drawn is that the release of mechanical boundary conditions is mainly elastic, and thus they can be modelled as removed at the same time. Furthermore, it is seen that the mechanical contact modelling is necessary to obtain reasonable results for some methods of preventing RBM.

The long plate is then studied, where the complete benchmark geometry is modelled. Using Chalmers Centre for Computation Science and Engineering (C3SE) one complete simulation is run in a reasonable time of 12 hours on 24 CPUs. The residual stresses and deformations are then extracted and compared to experimental data on angular distortion and deformations. It is found that the simplified modelling approach used can give good agreement for the residual stresses and for the shape of the residual deformations. The magnitudes of the residual deformations, though, are harder to predict.

Acknowledgements

We would like to express our gratitude to our supervisors who have been helpful and guided us throughout this project. A big thank you to Prof. Lennart Josefson (Chalmers University of Technology), Prof. Em Moyra McDill (Carleton University) and Shivaprasad Gurram for always being enthusiastic and eager to teach us as much as possible within this subject.

We would also like to thank Chalmers Centre for Computational Science and Engineering (C3SE) for providing us with a license to use PC-cluster Vera. This gave us the ability to perform all the necessary simulations within the timespan of this project. One simulation could take up to 6 days of CPU time to run in the computer room, a time that was massively reduced to a matter of hours, thanks to C3SE.

Table of Contents

1. Introduction 1
2. Project definition 2
2.1 Goals 2
2.2 Accomplishments 2
3. Method 3
3.1 Analytical calculations 3
3.2 Benchmark geometry 3
3.3 Assumptions 4
3.4 Simulations 5
3.5 Boundary conditions and load 8
3.6 Material data 9
3.7 Mesh and elements 10
4. Results 12
4.1 Short plate 12
4.1.1 Thermal simulations 12
4.1.2 Mechanical simulations 13
4.1.3 Key recommendations from the short plate 16
4.2 Long plate 16
4.2.1 Thermal simulation 16
4.2.2 Mechanical simulations and stresses 16
4.2.3 Mechanical simulations and measured deformation field 21
4.2.4 Mechanical simulations and measured distortion angles 23
4.2.5 Results from Group choice B and contact modelling 24
5. Discussion 26
5.1 Cooling time and thermal simulations 26
5.2 Tack release sequences and its effect on residual deformations 26
5.3 Rigid body motion and contact modelling 26
5.4 Residual stress state and comparison to experimental values on long plate 27
5.5 Measured deformation field compared to FE-simulations on long plate 28
5.6 Measured angular distortion compared to FE-simulations on long plate 28
6. Conclusion and recommendations to the ISSC benchmark 29
7. Future Work 30
References 31

List of Figures

1.1	(a) Sketch of benchmark geometry with $a = 80$ mm, $b = 400$ mm, $c = 5$ mm, $d = 1000$ mm, e are run-on/off tabs and (b) illustration of fillet a welding process.	1
3.1	Benchmark geometry along with the tack sequence between base plate and the table (1-6) [2].	4
3.2	ISSC method on short plate.	7
3.3	Group choice A on short plate.	7
3.4	Group choice B method of preventing RBM.	8
3.5	Sequential heating on long plate, with start at run-on tab, red shows the elements at weld temperature.	9
3.6	Effect of field variables in ABAQUS during first weld pass.	10
3.7	A validated mesh of the welded panel, (a) short plate (200 mm) and (b) long plate (1000 mm) [6].	11
4.1	Temperature during welding procedure with chosen settings of 1000˚C and 3 s.	13
4.2	Vertical displacement field [mm] on deformed plate, ISSC method (with and without the table).	15
4.3	Vertical displacement field [mm] on deformed plate, Group choice A method.	15
4.4	Nodal temperatures [˚C] before removal of tack welds.	16
4.5	Longitudinal residual stresses in base plate at the middle of the plate compared to experiment [4].	17
4.6	(a) Transverse residual stress state in the base plate and (b) the normal residual stress state in the base plate at the middle of the plate compared to experiment [4].	18
4.7	Longitudinal residual stress [MPa], in direction along the weld path.	19
4.8	Longitudinal residual stress inside of weld [MPa].	19
4.9	Transverse residual stress [MPa].	20
4.10	Transverse stress [MPa] at weld region.	20
4.11	Normal residual stress [MPa].	21
4.12	Normal residual stress [MPa] at weld region.	21
4.13	3D laser scanning of fillet welds [2] units in [mm].	22
4.14	Deformation field [mm] on long plate, ISSC RBM method.	22
4.15	Scheme for comparing deformations.	23
4.16	Angular distortions at locations 1 (1.29˚), 2 (1.40˚) and 3 (0˚).	24
4.17	Deformation fields on long plate.	25

List of Tables

3.1	Weld parameters for benchmark exercise [2].	3
3.2	Thermal simulations performed on 200 mm plate.	5
3.3	Mechanical simulations performed on 200 mm plate with different sequences of releasing tack welds.	6
3.4	Mechanical simulations performed on 200 mm plate with and without contact modelling.	6
3.5	Mechanical simulations performed on 1000 mm plate.	8
4.1	Thermal results for the short plate showing the selection of 1000˚C and 3 s.	12
4.2	Different sequences of releasing tack welds for short plate.	14
4.3	Contact modelling and RBM control.	15
4.4	Corner deformations [mm] on long plate, ISSC method.	23
4.5	Angular distortions [3] compared to angular distortions obtained from FE-simulation.	24
4.6	Corner deformations on long plate [mm], Group choice B.	25
4.7	Comparison between vertical displacements [mm].	25

1. Introduction

When constructing stiffened panels of a ship hull, welding techniques are generally used for welding stiffened panels onto a plate. In this project the welding process is assumed to be gas metal arc welding (GMAW). This welding process is such that molten material is deposited at a joint so that the edges of the plates are heated up and melted and thus joined together. Due to the local heating of edges, followed by rapid cooling of the weld material, residual deformations and stresses develop. One desired goal when designing different types of ships is to lower the weight of the ship hull, by reducing the thickness of the stiffened panels in the hull. One of the positive aspects of weight reduction is that the loading capacity during transportation can be increased. Furthermore, the material reduction is also of importance due to economic and environmental aspects. This reduction though, can lead to some complications because of the welding process. Examples of this include assembly issues, risk of buckling of the panel and reduced fatigue strength.

This project is a part of the Masters programme Applied Mechanics at Chalmers and will also contribute to a benchmark exercise in a Specialist Committee, V.3 Materials and Fabrication Technology for the International Ship and Offshore Structures Congress (ISSC) 2022 Conference [1]. The aim of this project is to adapt existing finite element models (FE-models) to study residual stresses and deformations on a specific benchmark geometry [1,2] and to find out what simplifications that can be made in the modelling. The benchmark geometry is shown in Figure 1.1. Tack welds can be seen at the corner and mid-sides.

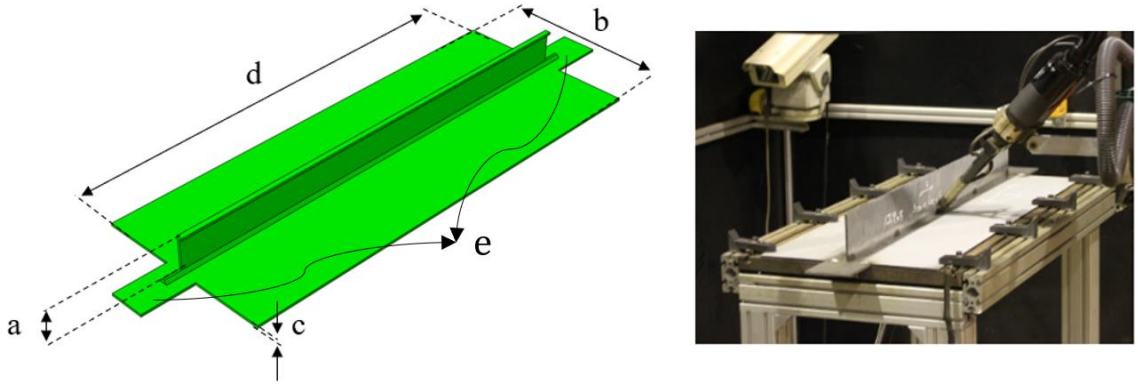

(a) Sketch of benchmark geometry **(b)** Set up of fillet welding case

Figure 1.1. (a) Sketch of benchmark geometry with $a = 80$ mm, $b = 400$ mm, $c = 5$ mm, $d = 1000$ mm, e are run-on/off tabs and (b) illustration of fillet a welding process.

The simulations are initially carried out on a short plate (200 mm) to be able to draw conclusions by reducing the computational complexity when compared to the long plate (1000 mm). In both these models the tack welds positioning the stiffener to the plate are omitted, and only the tack welds seen at the corners and mid-sides of the plate in Figure 1b are modelled. Furthermore, the run-on and run-off tabs seen in Figure 1.1, are only modelled for the long plate and not for the short plate.

2. Project definition

Under this section the project is discussed in terms of the goal that was set up, and also which goals that were accomplished during the project.

2.1 Goals

The goal of the project is to develop and analyse a simulation procedure for two-pass fillet welding of a stiffener to a plate for predicting residual deformations and stresses. These will be compared to experimental results [3,4] as a contribution to the specialist committee. Recommendations will be made to the ISSC benchmark committee on simplifications that can be exploited in the modelling of two-pass fillet welding of a stiffener to plate.

2.2 Accomplishments

Project specific deliverables that have been accomplished during this project are listed below. These deliverables have been necessary to reach the goal of this project:

1) Analytical calculations based on text-book solutions have been performed to obtain a range for the cooling time between 800˚C and 500˚C in the weld after the weld has been deposited at a certain temperature.
2) The temperature gradients from the FE-results have been compared to the analytical range and the FE-models have been adapted accordingly to obtain the best parameters to describe the simplified heat source model.
3) (a) Forward-coupled thermal-mechanical FE-simulations have been performed on a short (200 mm) plate and adapted for the purpose of this project.
   (b) Different sequences of removing tack welds on a short (200 mm) plate have been tested using FE-simulations, to see the effects of releasing tack welds on the final residual deformations.
   (c) Different methods of preventing rigid body motion (RBM) have been studied to see the effects of these methods on the deformations on the short plate.
4) Choices from short plate best combinations from simplified modelling of heat source, sequence, (add conclusions)
5) Forward-coupled thermal-mechanical FE-simulations have been performed on a long (1000 mm) plate.
6) Different methods of preventing RBM have been studied on the long plate, as well as the effect of modelling contact or not.
7) Residual stresses, deformations, and distortion angles on the long plate have been compared to experimental data.
8) Recommendations on how to model two-pass fillet welding of a stiffener to plate for the ISSC benchmark have been made.

3. Method

3.1 Analytical calculations

The weld parameters for the GMA weld process that are specific to the benchmark exercise are specified in Table 3.1.

Table 3.1. Weld parameters for benchmark exercise [2].

Weld parameters		
Weld process	GMAW	Symbol
Welding speed	0.59 [m/min]	v
Wire feed rate	9.0 [m/min]	
Current	250 [A]	I
Mean voltage	29 [V]	U
Estimated arc efficiency	0.7	η

With these parameters an analytical cooling time can be calculated between $800˚\text{C}$ (1073K) and $500˚\text{C}$ (773K) for a welding configuration of a moving heat source on a plate, with a point heat source, q, and a constant velocity v (m/s). For a thin plate the cooling time, Δt (s), is given by the following equations in [5]:

$$\Delta t = \frac{\left(\frac{q}{v}\right)^2}{4\pi\lambda\rho c\theta_2^2 d^2} \tag{1}$$

$$\frac{1}{\theta_2^2} = \frac{1}{(773 - T_0)^2} - \frac{1}{(1073 - T_0)^2} \tag{2}$$

Where $q = UI\eta$ is the heat input (W), λ the thermal conductivity ($\text{Jm}^{-1}\ \text{s}^{-1}\ \text{K}^{-1}$), ρ the density (kgm^{-3}), c specific heat ($\text{Jkg}^{-1}\text{K}^{-1}$) and d is the thickness of the plate (m), T_0 is the room temperature (˚C). The cooling time between $800˚\text{C}$ and $500˚\text{C}$ for a specific welding process, geometry and material will be constant within this range as described in [5]. The temperature $800˚\text{C}$ is important for a weld, since in most steels it represents the A_3 transformation temperature from austenite. This $800˚\text{C} - 500˚\text{C}$ temperature interval is widely used to characterize the welding process since it encompasses the major metallurgical changes [5].

Since the material properties are temperature dependant no exact value can be obtained from these equations. Instead, a range can be obtained by using material data for thermal conductivity and specific heat at different temperatures such as room temperature and $500˚\text{C}$ so that a range that characterises the weld can be found.

3.2 Benchmark geometry

The benchmark geometry is described in full detail in [2] and consists of a stiffener that is welded onto a plate as seen in Figure 1. Both the plate and the stiffener are made out of DH36 steel and have the dimensions $(1000\ x\ 400\ x\ 5)$ mm and $(1000\ x\ 80\ x\ 5)$ mm, respectively. The base plate and stiffener are welded together perpendicular to each other,

by GMAW. Initially 5 tack welds, shown as small dots in Figure 3.1, were used in the benchmark to temporarily position the stiffener to the plate. The plate is placed on a table and is kept there by a set of tack welds at six points as seen in Figure 3.1.

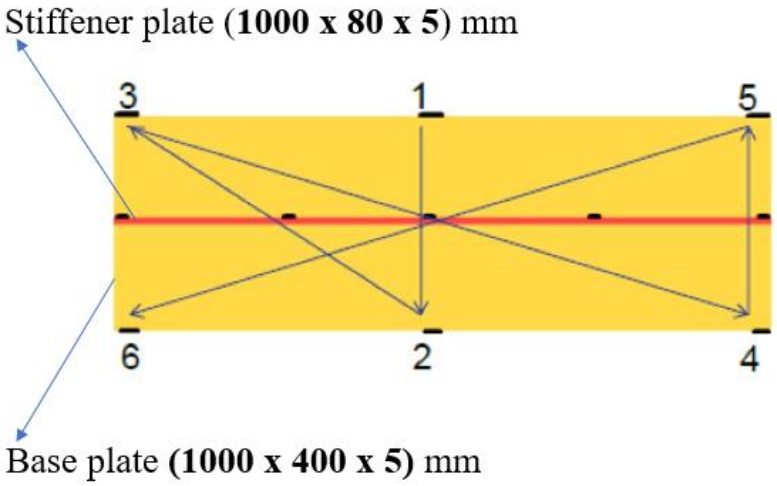

Figure 3.1. Benchmark geometry along with the tack sequence between base plate and the table (1-6) [2].

The welding process consists of two weld passes in opposite direction. Once the first pass is cooled, the second pass is made. After the second pass, when the weld has reached a temperature less than 60°C, the six tack welds holding the plate to the table are cut off and the released plate then deforms.

3.3 Assumptions

In this section model assumptions are listed that can affect the results in some way. These assumptions can range from how the heat source is modelled to how the table beneath the plate is modelled.

- The modeling of the moving heat source, generated from the welding process, is modelled as a stepwise heating of elements by prescribing nodal temperatures to a fixed maximum value.
- It is assumed that heat is generated by the weld and not by possible plastic deformation, allowing a forward-coupled thermal-mechanical FE-model to be used.
- Effects from phase transformations from austenite to pearlite/ bainite / martensite are not included in the constitutive modeling.
- A weld in not uniform, however in the FE-model used the cross section of the weld is triangular with the same dimensions along the plate.
- The table is modelled as a surface limited to under the surface only. In reality, the plate can deflect and have contact with the table at more locations. However, this will not be seen in the FE-model. For some simulations, the contact is completely neglected, meaning that the plate is hanging at the tack welds only. How this affects the results will be studied in this project.

3.4 Simulations

The FE-simulations have been carried out using a forward-coupled thermal-mechanical FE-analysis to simulate the welding process [6], with material and geometrical nonlinearity incorporated. As will be shown below, the thermal model has been validated by comparison to analytical solutions. The thermal-mechanical model has been validated by comparison to experimental results for angular distortion and separately residual deformations and stresses. No use of symmetry has been employed, since the two-pass fillet welding is not a symmetric process.

In the thermal FE-model a heat source has been added element-wise in a step-wise fashion of heating and cooling, simulating an actual welding process [6]. To further simulate an actual welding process where the material is added gradually, inactive elements with low conductivity and an elastic modulus of 100 [MPa] have been used on the weld region, which were then assigned the weld material properties once they reached a prescribed temperature. The result from this simulation was then used as input to the mechanical model as a predefined temperature field with nodal temperatures [6]. The mechanical model then simulated the removal of the tack welds and calculated the residual stresses and deformations on the plate. Using simulations, the optimal time interval for sequential heating has been found by comparing results with analytical solutions regarding temperature gradients. After this time interval had been found, the FE-models have been adapted to fulfil this time interval. The adapted FE-model was then used to study different sequences of releasing the tack welds that hold the plate against the table. The optimal way of releasing the tack welds, to limit residual deformations was then found. Furthermore, the effects of contact modelling have also been studied considering a table beneath the plate, together with different methods of preventing rigid body motion (RBM). Other ISSC participants have used springs to prevent RBM, which was not studied in the current project.

Results from the short (200 mm) plate, were then used on a longer (1000 mm) plate. By studying the longer plate, the residual stresses and deformations can be calculated and compared to experimental results.

The simulations that have been performed were divided into thermal and mechanical simulations. In Table 3.2, the simulations used to study the optimal cooling time are numbered. Here the welding speed and maximum temperature were altered. The welding speed can be changed somewhat because of some uncertainty with the arc efficiency [7].

Table 3.2: Thermal simulations performed on 200 mm plate.

Thermal simulations (short plate)		
Step time [s]	Maximum temperature [˚C]	Simulation number
4	1300	1
4	1200	2
4	1000	3
2.8	1000	4
3	1000	5
5	1000	6
5.2	1000	7

The sequential heating representing the weld was divided into a number of steps for each weld on each side of the stiffener. By altering the step time, the speed of the weld could be changed. In Table 3.3 the mechanical simulations necessary to study the effect of different sequences of releasing tack welds, are listed.

Table 3.3: Mechanical simulations performed on 200 mm plate with different sequences of releasing tack welds.

Mechanical simulations (short plate)		
Sequences	Simulation number	Contact modeling
Counterclockwise	8	YES
Diagonal pattern	9	YES
Simultaneously	10	YES
Two by two	11	YES

To also be able to study the effect of contact modelling of a table beneath the plate, an additional set of simulations was performed, that are seen in Table 3.4. When the contact conditions were removed, the plate essentially hangs in the tack welds as its only support. For this simulation setting inertia relief [8] for preventing RBM was also studied.

Table 3.4: Mechanical simulations performed on 200 mm plate with and without contact modelling.

Mechanical simulations (short plate)			
Sequences	RBM method	Simulation number	Contact modeling
Counterclockwise	Group choice A	12	YES
Counterclockwise	Group choice A	13	NO
Counterclockwise	Inertia relief	14	NO
Counterclockwise	ISSC method	15	YES
Counterclockwise	ISSC method	16	NO

The ISSC method [2] for preventing RBM after tack weld release was used for two of the simulations. In this method one corner should be locked in all degree of freedom (3 dof), one corner is locked normal to and along the base plate (2 dof) to prevent rotations, and a third corner is locked only normal to the base plate (1 dof) to prevent rotation. This is seen in Figure 3.2 where the 6 dof are indicated by black arrows.

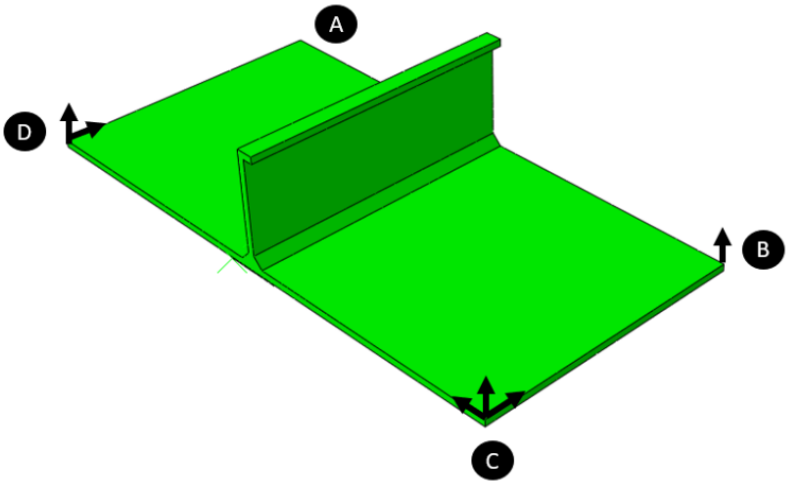

Figure 3.2. ISSC method on short plate.

The inertia relief feature was also tested, which is a load applied on the whole model to balance externally applied forces, preventing RBM.

Since the ISSC method fixed three corners vertically and was unrealistic a third method called Group choice A was developed. It also involves 6 dof: one corner is also locked in all three directions, one corner in the plane of the base plate and one corner only along the base plate[1]. This method is visualised in Figure 3.3. In contrast to the ISSC method this method allows for three corners to move more freely in the vertical.

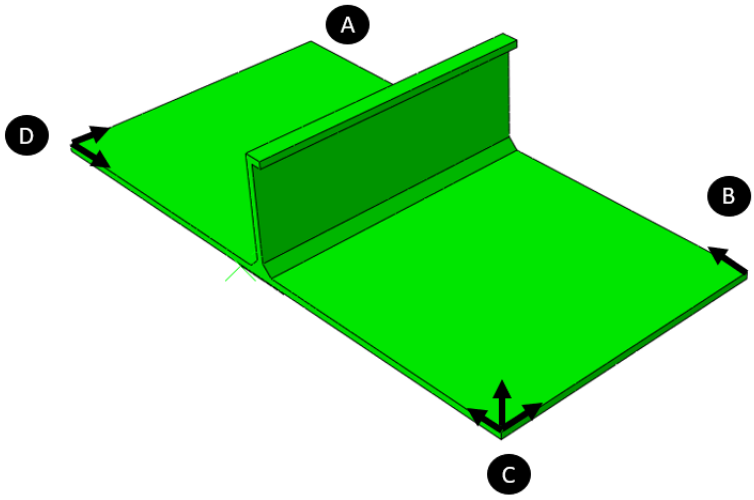

Figure 3.3. Group choice A on short plate.

Finally, when the simulations for the short plate had been performed and selections made, the long plate was considered. The set of simulations, and different settings for these simulations can be seen in Table 3.5. Here the ISSC approach was used since it was a recommended approach, however an additional method was also tested called Group choice B. In Group choice B, 6 dof are locked as indicated by Figure 3.4 for the short

[1] This is normally referred to as the 3-2-1 method dealing with RBM.

plate. In this method the corners are freer to move vertically in contrast to the ISSC method. This has a possibility of capturing the real deformations of the plate in a better way.

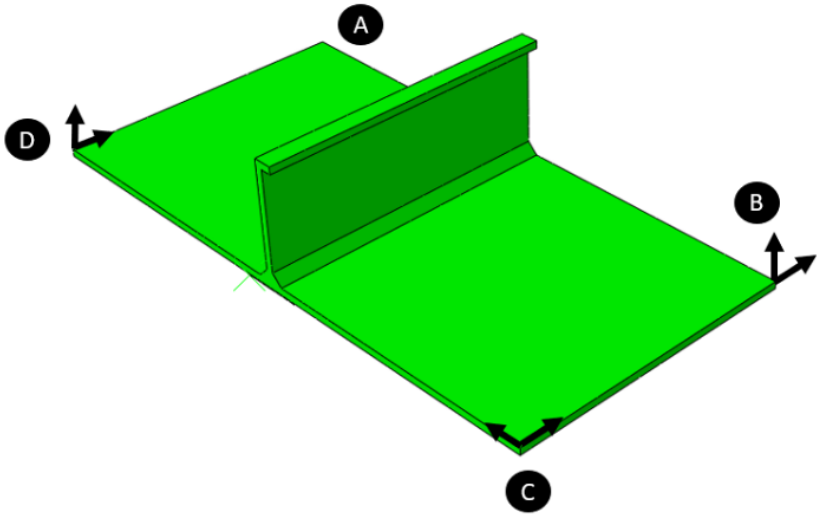

Figure 3.4: Group choice B method of preventing RBM.

To see the effect of contact modelling, one simulation for the long plate was also run with the contact deactivated as seen in Table 3.5.

Table 3.5: Mechanical simulations performed on 1000 mm plate.

Mechanical simulations (long plate)			
Sequences	RBM method	Simulation number	Contact modeling
Counterclockwise	ISSC method	17	YES
Simultaneoulsy	ISSC method	18	YES
Counterclockwise	Group choice B	19	YES
Simultaneoulsy	Group choice B	20	YES
Counterclockwise	Group choice B	21	NO

3.5 Boundary conditions and load

Thermal and mechanical boundary conditions were required for the forward-coupled FE-analysis.

The thermal boundary conditions were divided into several types of boundary conditions. The Dirichlet part consist of the weld area where the nodal temperatures were prescribed so that the nodes in the weld path are given a specific temperature (maximum 1000°C up to 1300°C). Furthermore, the Newton (convection boundary condition) part of the boundary consists of the area in contact with the air in the room, where the room temperature was prescribed to 20°C. The last part of the boundary consists of the bottom area of the plate in contact with the table, where heat conduction at constant room temperature occurs [6].

The weld area has been prescribed nodal temperatures in a sequential manner that consists of 5 steps for each weld pass for the short plate and 27 steps for each weld pass on the long plate. Figure 3.5 shows the first heating step on the run-on tab.

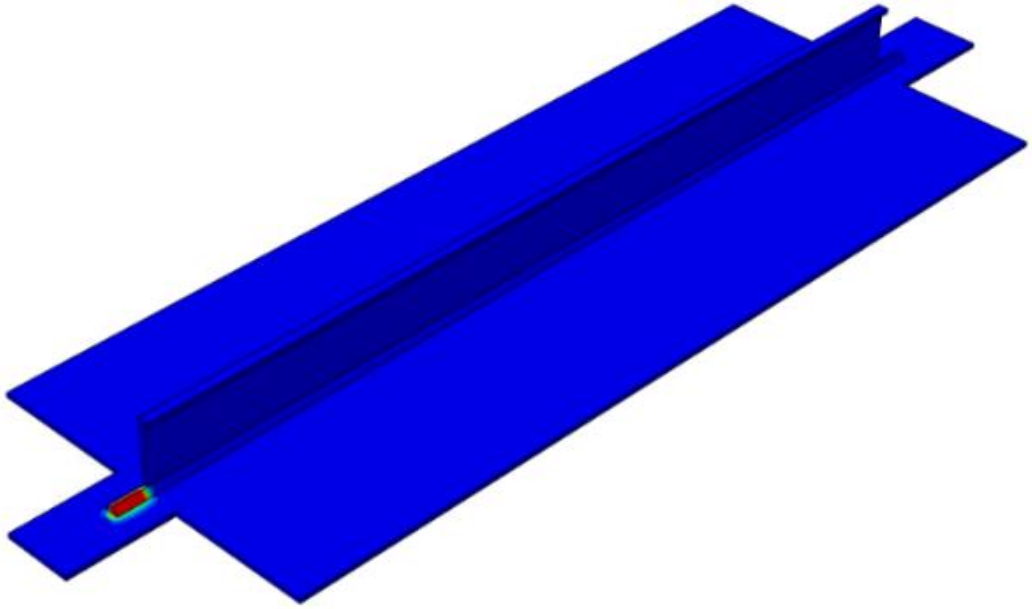

Figure 3.5. Sequential heating on long plate, with start at run-on tab[2], red shows the elements at weld temperature.

The mechanical boundary conditions for the short plate (200 mm) consisted of the tack welds at each corner of the plate [6], this is a Dirichlet type boundary condition where the degrees of freedom were first locked in all directions. For the long plate (1000 mm) the tack welds located as in Figure 3.1, with tack welds also in the middle. These nodes have been chosen as six nodes at each corner, such that in total 24 nodes were locked in the short plate, and 36 nodes for the long plate. During the release of tack welds, these boundary conditions were deactivated in a sequence of steps.

Contact conditions beneath the plate to model the table have also been used. This method is based on Lagrange multipliers which will create a hard contact in contrast to e.g. penalty. The modelled table is limited to an area close to the stiffener. Additionally, the tack welds that are initially used in the benchmark exercise to position the stiffener to the plate when welding, was not considered, only the tack welds fastening the plate to the table have been considered.

3.6 Material data

This project is part of a benchmark exercise and the specified material is DH36 steel, however most of the material data used in this project is a steel with similar properties, namely S355 [2]. However, the specific heat and also the thermal conductivity could be obtained for the actual steel, DH36 [2]. The material properties have been imported to ABAQUS via an input file that contains the temperature-dependent data used in this

[2] Run-on and run-of tabs are used to improve the start and stop heat flow and reduce the formation of defects associated with the welding process.

project. The constitutive model used in the FE-analysis is discussed in [6] where the constitutive modelling has been implemented for the benchmark exercise.

To simulate that the material from the welding rod is added successively, inactive weld elements ahead of the weld were given a low conductivity and stiffness. This was done in ABAQUS with field variables, which are illustrated in Figure 3.6 below. In Figure 3.6 it is clearly seen that the conductivity has been set to 0 on the not yet activated weld on the left side, since no heat is conducted to this region whilst it is conducted to other areas of the base plate.

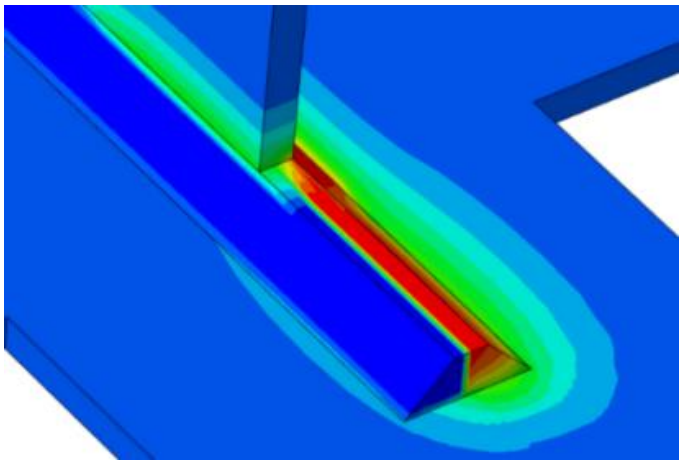

Figure 3.6. Effect of field variables in ABAQUS during first weld pass.

3.7 Mesh and elements

The mesh used for the forward-coupled thermal-mechanical analysis of the shorter plate is shown in Figure 3.7 (a). The mesh has previously been subjected to a convergence study in [6] and further work has been performed afterwards so that it was determined to be regarded adequate [4]. The elements used for the thermal simulations were 8-node linear heat transfer brick elements (DC3D8) and 6-node linear heat transfer triangular prism elements (DC3D6), whilst for the mechanical simulations 8-node linear brick elements (C3D8) and 6-node linear triangular prism elements (C3D6) were used, described in the ABAQUS manual [9]. The total number of C3D8-elements was 7650 and the total number of C3D6-elements was 2150 for the short (200 mm) plate.

The same element types were used for the long plate (1000 mm), as seen in Figure 3.7 (b). For the long plate in total 58756 elements were used.

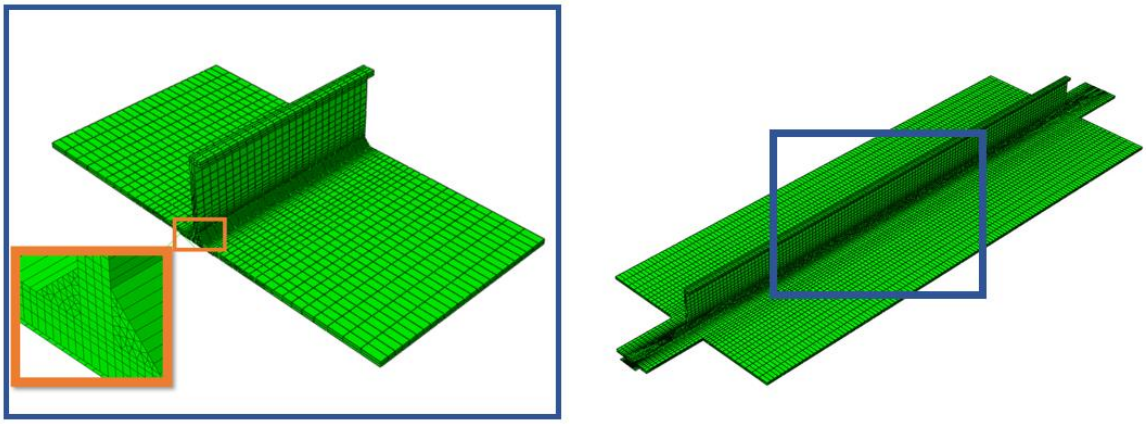

(a) Mesh on short plate **(b)** Mesh on long plate

Figure 3.7. A validated mesh of the welded panel, (a) short plate (200 mm) and (b) long plate (1000 mm) [6].

4. Results

In this section results are presented and discussed in terms of decision points determined using the shorter model. First the results from the short plate are presented, divided into results from thermal and mechanical results separately. This section is followed by results from the long plate, also divided into results based on thermal and mechanical simulations.

4.1 Short plate

Thermal and mechanical results for the short plate are presented and choices identified for further analyse.

4.1.1 Thermal simulations

The analytical cooling range between 800˚C and 500˚C was found, using the equations in section 3.1, to be between 4.9 s and 6.7 s, based on the material properties for DH36 [2]. To find an optimal value in the middle of this range, seven simulations with different settings were performed. First, three simulations were done with three different temperatures with the actual weld speed 0.59 m/s. These simulations showed that the cooling time gets closer to the analytical range when the maximum temperature is 1000˚C instead of 1200˚C or 1300˚C, shown in Table 4.1.

It was decided that 1000˚C would be the standard for thermal simulations. To further improve the cooling time, the weld speed can be altered because of an uncertainty with the arc efficiency [7]. Changing the step time for each of the 10 heating steps for the two weld passes, was thus done. This showed that the optimal step time for heating was 3 s which, together with the maximum temperature of 1000˚C, gave a cooling time of 6 s. This value is in the middle of the analytical range and was chosen to be the optimal setting for further simulations. The results are shown in Table 4.1.

Table 4.1. Thermal results for the short plate showing the selection of 1000˚C and 3 s.

Cooling time [s] 800 -> 500	11	10	7	
Step time heating [s]	4	4	4	
Maximum temperature [˚C]	1300	1200	1000	
Analytical range (4,9-6,7) [s]			√	
Cooling time [s] 800 -> 500	5	6	8	9
Step time heating [s]	2.8	3	5	5.2
Maximum temperature [˚C]	1000	1000	1000	1000
Analytical range (4,9-6,7) [s]		√		

The temperature at one node at the middle of the plate, at the weld centerline is studied in Figure 4.1. Here the nodal temperature is seen for the complete weld procedure. The studied time interval between 800˚C and 500˚C is seen in the beginning of the procedure.

As seen the maximum temperature is 1000˚C, and the lowest somewhere near 40˚C. The second peak is a result of the second weld pass on the other side of the siffener.

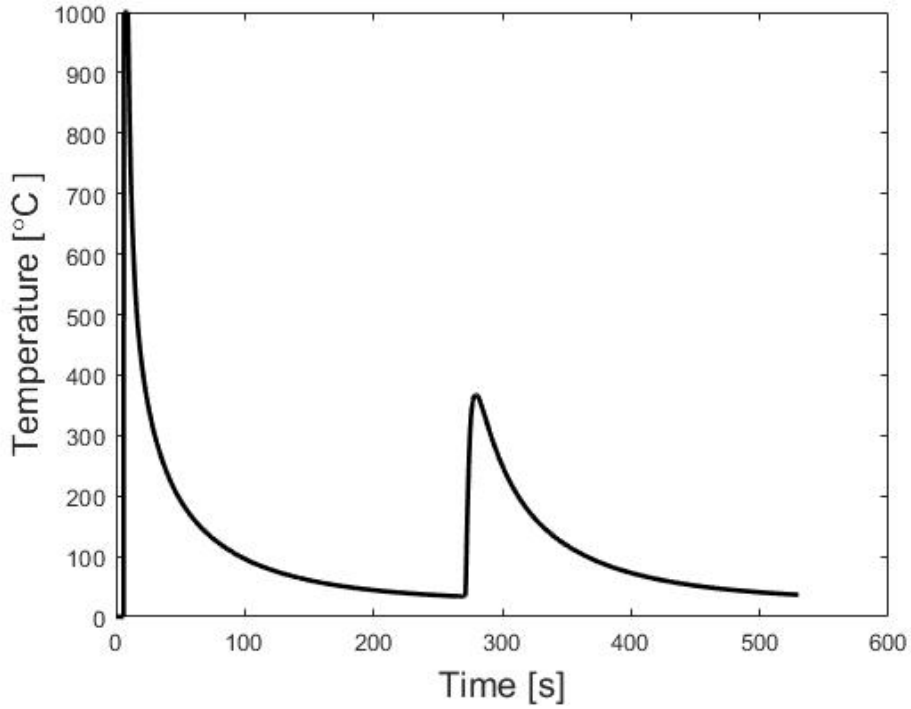

Figure 4.1. Temperature during welding procedure with chosen settings of 1000˚C and 3 s.

4.1.2 Mechanical simulations

With the settings decided in the previous section the mechanical simulations were performed. First a comparison of different sequences for removing the tack welds, holding the plate to the table when welding, was considered. This comparison was based on the displacements normal to the base plate at the four corners of the base plate, numbered as in Figure 3.2 from A to D. The results from these simulations are shown in Table 4.2.

For options were considered:

- Releasing the tack welds counterclockwise (c.c), starting at corner B, one tack weld at a time.
- Releasing the corners diagonal each other.
- Simultaneous release of all tack welds.
- Release of two tack welds at a time (2 by 2), on the opposite short sides.

Table 4.2. Different sequences of releasing tack welds for short plate.

Short plate				
Corner vertical dicplacements [mm]				
A	4.77	4.77	4.3	4.94
B	-0.03	-0.03	-0.02	-0.07
C	0	0	0	0
D	5.57	5.55	5.2	5.62
Sequence:	c.c	diagonal	simultaneous	2 by 2
	√			

The results showed that the sequence of releasing tack welds did not change the deformations to any large extent. However, the smallest deformations were obtained from releasing all tack welds simultaneously, even though the difference was small. The conclusion that was drawn from this was that the release sequence did not matter. Possibly this might occur because the removal of tack welds does not cause any plastic deformation. However, one sequence has to be chosen to remove the tack welds. The counterclockwise release sequence was chosen since it is most realistic to release the tack welds in this fashion after an actual welding process where the welder can walk around the plate, cutting one tack weld at the time. Alternatively, the simultaneous sequence could have been chosen to simplify the model by reducing the number of simulation steps.

Second, the simulations were run with or without modelling contact to see if the table beneath the stiffener is necessary or not. Removing the contact modelling could significantly reduce the computational cost and was an interesting factor to look at. This was done using three different methods of preventing RBM as the tack welds are released. The results in Table 4.3 show the five combinations considered as discussed in 3.4. in terms of displacements at the corners.

It can be seen that the ISSC method completely locks the nodes in the direction normal to the base plate at three locations, while the Group choice A method is only locked in this direction at one corner, and the inertia relief method is completely free at all corners.

The results show that modelling including the table is necessary for the Group choice A method since, without the table, the displacements are unrealistic. Inertia relief could only be used in ABAQUS without contact conditions. The result of this method was also abnormal displacements and hence this method disregarded. This result may be because there is no modelling of the table included. For the ISSC method the contact modelling does not seem to matter, at least in terms of the displacements at the corners. Other behaviours may be lost when not having the table modelled, thus it was decided to keep the table for further investigations if it is decided to study different methods for preventing RBM.

Table 4.3. Contact modelling and RBM control.

Short plate					
Corner vertical dicplacements [mm]					
A	5.15	49.5	2.22	2.22	14
B	0.1	-21	0	0	-3
C	0	0	0	0	-2
D	5.58	55.9	0	0	13
Contact:	Table	No table	Table	No table	No Table
RBM control	Group choice A	Group choice A	ISSC method	ISSC method	Inertia relief

The deformed mesh, with the vertical displacement field, is shown for the ISSC method with contact modelling in Figure 4.2 for reference.

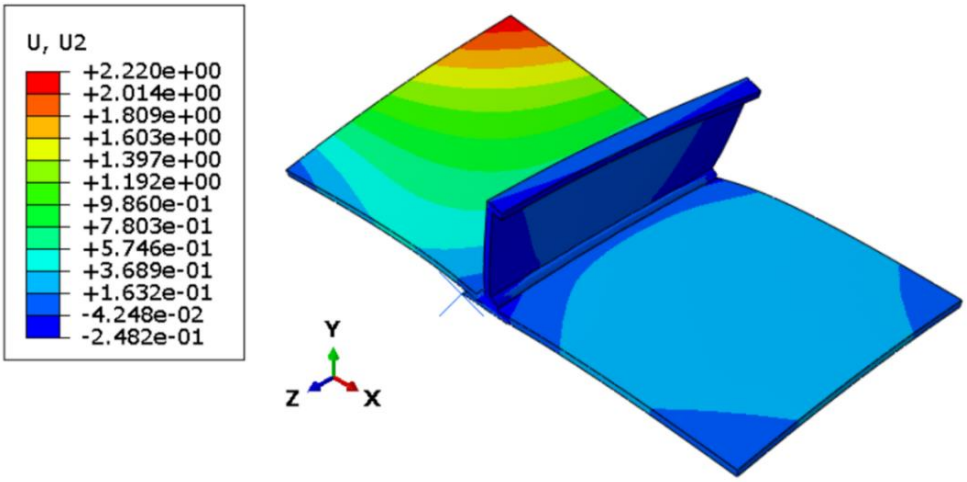

Figure 4.2. Vertical displacement field [mm] on deformed plate, ISSC method (with and without the table).

Similarly for the Group choice A method, the vertical displacement field can be seen in Figure 4.3. The corner displacements are as mentioned seen in Table 4.3.

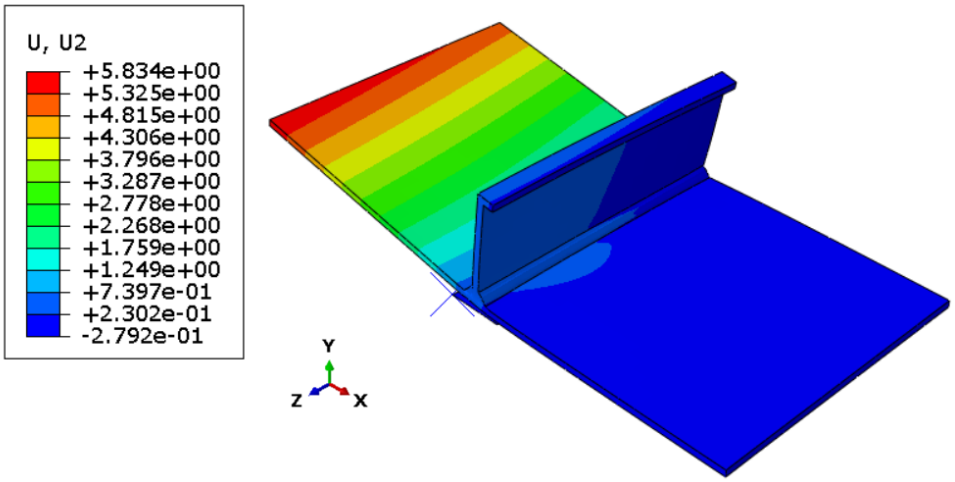

Figure 4.3. Vertical displacement field [mm] on deformed plate, Group choice A method.

4.1.3 Key recommendations from the short plate

The key results that go forward to the long plate are listed below:

- The maximum temperature should be set to 1000˚C.
- The step time for heating should be set to 3 s.
- The table should be included.
- The sequence of releasing the tack welds does not matter for the short plate, however a counterclockwise sequence and a simultaneous release of tack welds are used for the long plate.

4.2 Long plate

The results obtained from the simulations of the long plate are presented in the following section, divided into thermal and mechanical simulations, respectively. As stated above, the short plate gave valuable results that can now be incorporated.

4.2.1 Thermal simulation

To verify that the simulations follow the benchmark exercise the thermal simulation is first studied. As mentioned in the method, the weld temperature must be below 60˚C everywhere in the weld regions. The nodal temperature field after cooling, before the removal of tack welds are seen in Figure 4.4. This simulation has been made with the thermal settings decided to be optimal, i.e. 1000 ˚C and a step time for heating of 3 s for each of the 27 heating steps for each weld pass.

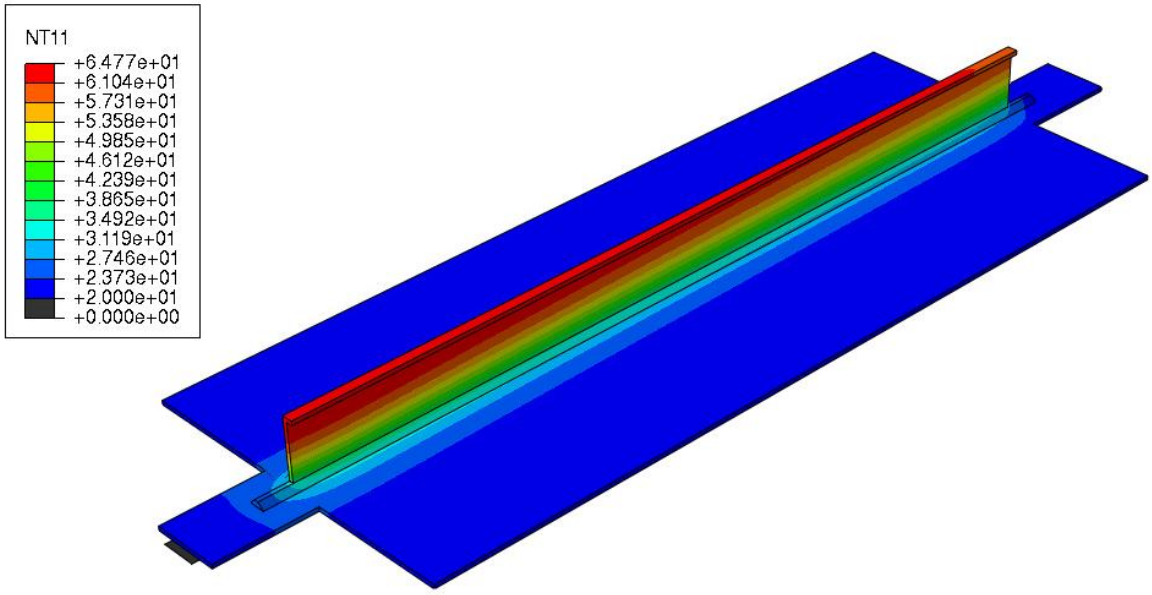

Figure 4.4. Nodal temperatures [˚C] before removal of tack welds.

In Figure 4.5 it is seen that the temperature in the weld is well below 60˚C. This temperature is only present at the top of the stiffener, as was the case for the short plate. Clearly the thermal settings for the short plate are also applicable for the long plate.

4.2.2 Mechanical simulations and stresses

The mechanical simulations for the long plate were made with the ISSC method for preventing RBM. Two different sequences for releasing the tack welds have been used:

first a counterclockwise release sequence, and secondly a simultaneous release of the tack welds. Once the tack welds holding the plate to the table have been released, the residual stress fields can be obtained for the long plate. The residual stresses can be divided into: longitudinal residual stresses, in the direction along the weld; transverse residual stresses, in the direction transverse the base plate and also normal residual stresses in the direction normal to the base plate. Experimental data for these stresses exist for the base plate, in the middle of the plate at the thickness 2.5 mm into the 5 mm thick base plate. The experiments have been conducted on a 200 mm long plate with a width of 200 mm, with run-off and run-on tabs [4]. The residual stresses have been measured after the two weld passes have passed.

In Figure 4.5 the longitudinal stress in the base plate is plotted with results from the FE-simulations and from experiments. The horizontal axis is limited to the range where experimental data exists. Since it turned out that both the residual stresses and deformations are the same for both release sequences of removing tack welds, they are from now on only referred to as one FE-simulation. Good agreement is seen between experimental data and FE-simulation. There is tension where the welds are located and compressional stresses further out from the weld. These stresses then balance each other out. Also, the amplitudes are approximately the same with a maximum longitudinal stress at about 400 MPa.

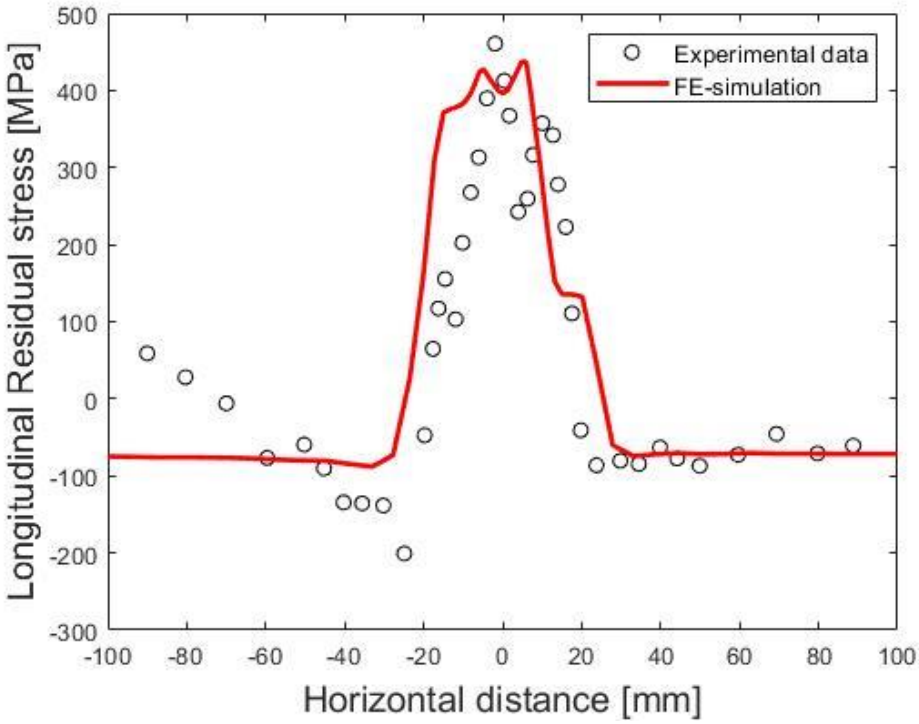

Figure 4.5. Longitudinal residual stresses in base plate at the middle of the plate compared to experiment [4].

The transverse residual stresses are seen in Figure 4.6 (a) with results from both experiments [4] and FE-simulations. Here there are larger differences between the experimental results and the result from FE-simulation. However, the general pattern is the same with almost constant stress along the base plate. The amplitudes for the

transverse stresses obtained from both methods, are distinctively lower than the longitudinal stresses.

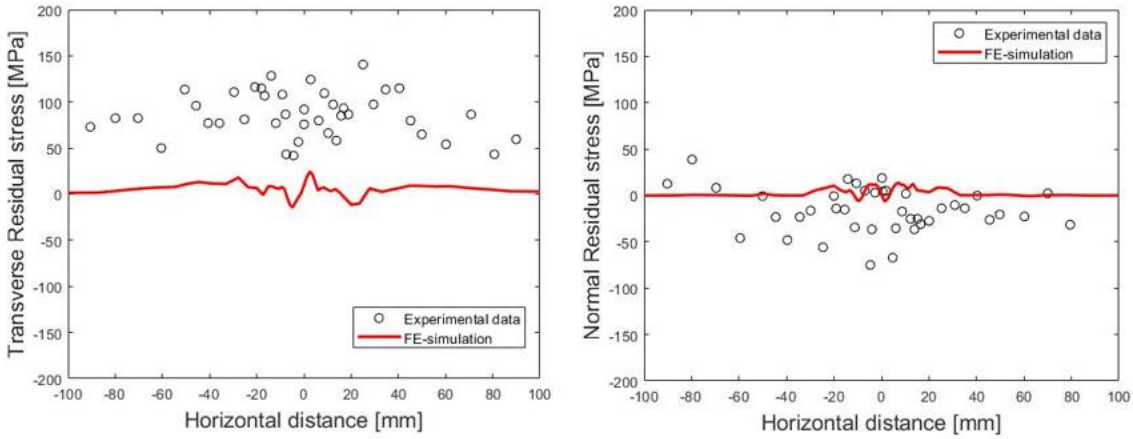

(a) Transverse residual stress (base plate) **(b)** Normal residual stress (base plate)

Figure 4.6. (a) Transverse residual stress state in the base plate and (b) the normal residual stress state in the base plate at the middle of the plate compared to experiment [4].

Lastly, the normal residual stresses are seen in Figure 4.6 (b), again with results from both FE-simulations and experiments. A similar pattern is seen for both the experimental and simulation data, with almost constant stresses along the base plate. Here it is confirmed that the longitudinal stresses are the highest of all three stresses, for both experimental data and simulation data.

To get a better understanding of the stress distribution, residual stress fields can be studied as well. In Figure 4.7 the longitudinal stress is seen on the deformed mesh after employing ISSC method of preventing RBM. As can be seen the stresses are the highest at the weld region, and smaller at the outer regions of the plate. The longitudinal stress at the weld region is somewhere around 750 MPa but at some points approach 1270 MPa.

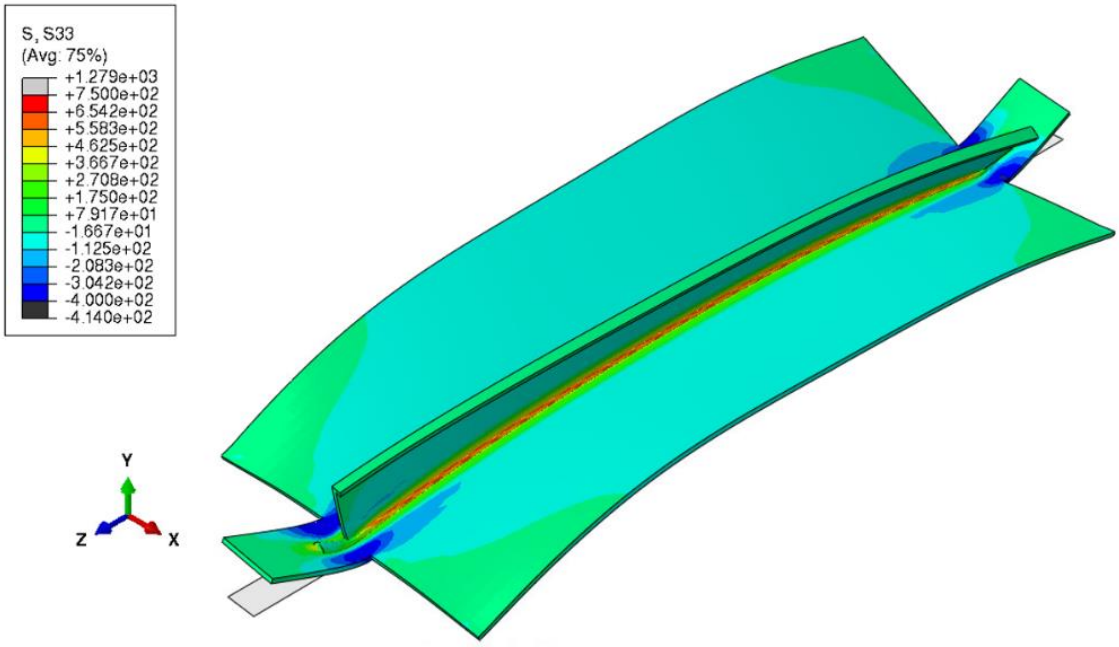

Figure 4.7. Longitudinal residual stress [MPa], in direction along the weld path.

To study these stresses in more detail, a cut at the middle of the plate is presented in Figure 4.8. This figure shows the longitudinal stresses inside the weld as well.

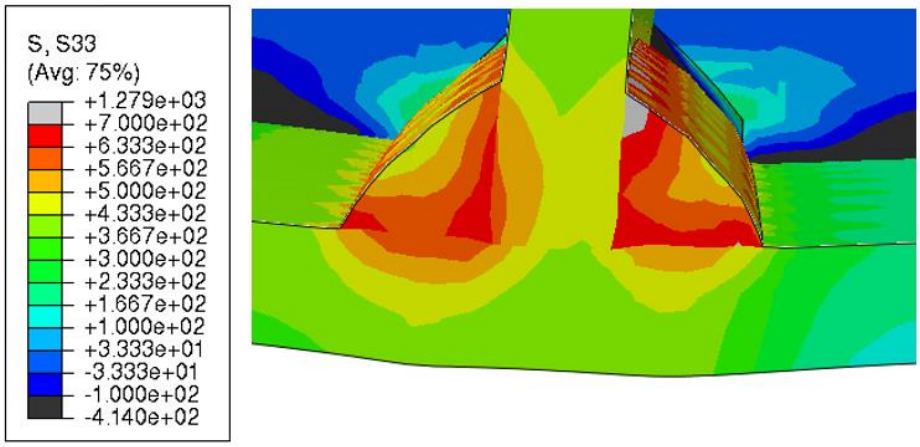

Figure 4.8. Longitudinal residual stress inside of weld [MPa].

Here it is once again seen that the longitudinal stress in the weld is usually around 400 MPa to 700 MPa, with some points along the weld where the stress reaches values around 1000 MPa. Furthermore, the transverse residual stress in seen in Figure 4.9. The transverse stress is at maximum about 600 MPa, however it is mostly in the range 25 MPa to 200 MPa.

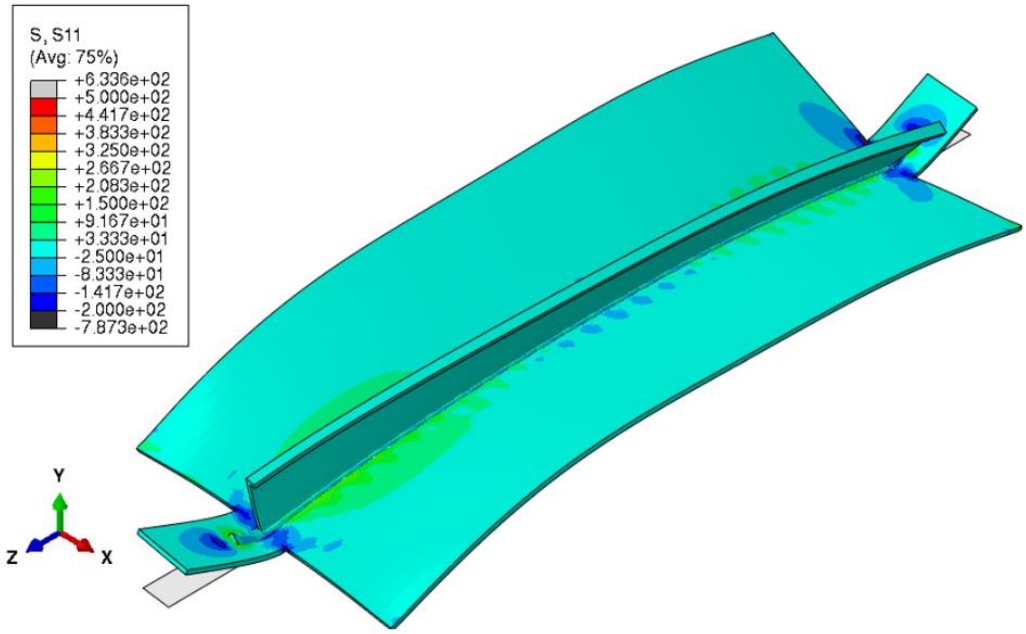

Figure 4.9. Transverse residual stress [MPa].

To see the transverse stresses more clearly a zoom in at the weld region is seen in Figure 4.10. The maximum value is about 600 MPa and the minimum value about −800 MPa. The black region in the outer area of the left weld stands out in contrast to the overall stress field.

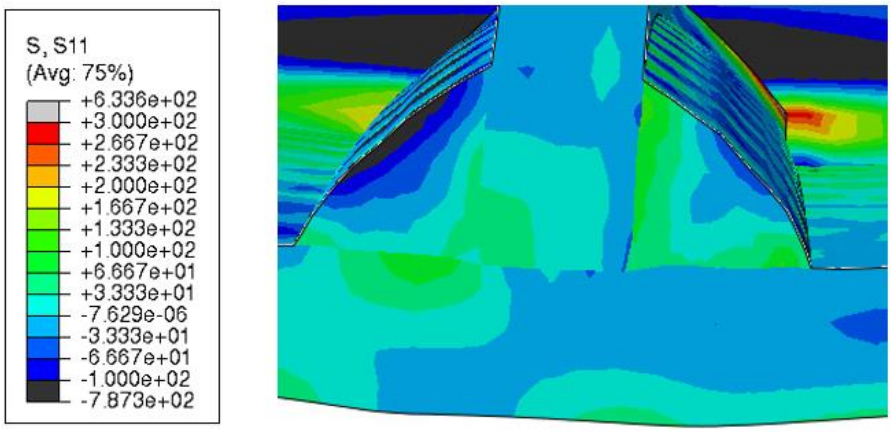

Figure 4.10. Transverse stress [MPa] at weld region.

In Figure 4.11 the normal residual stress is seen, with most values close to zero. However, at the weld region, the stresses can go up to about 700 MPa and down to -700 MPa.

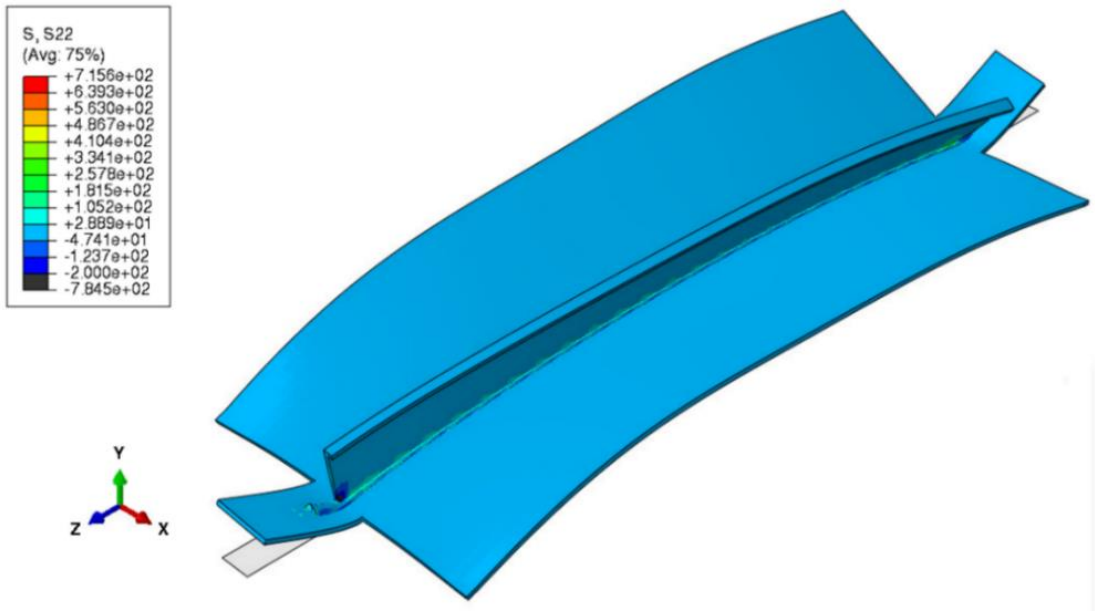

Figure 4.11. Normal residual stress [MPa].

To see the normal residual stresses more clearly a zoom in at the weld region is seen in Figure 4.12. Here the same pattern is seen as for the transverse stresses, where the outer area of the left weld has a value distinctively different from the overall stress field.

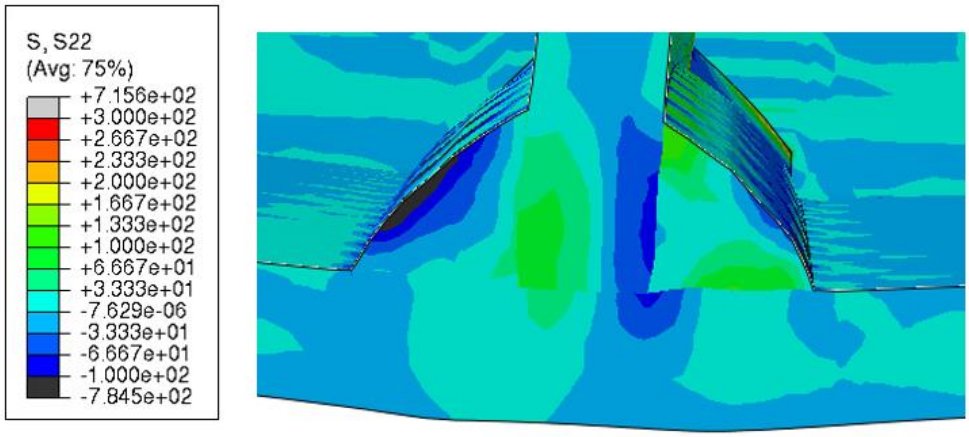

Figure 4.12. Normal residual stresses [MPa] at weld region.

4.2.3 Mechanical simulations and measured deformation field

The most important part of the ISSC benchmark is to consider the deformation field of the welded panel. Experimental results for the long plate exist for the deformation field [2]. These measurements were obtained from laser scanning and the result is seen in Figure 4.13. At different locations on the plate, the displacements normal to the base plate are seen in mm.

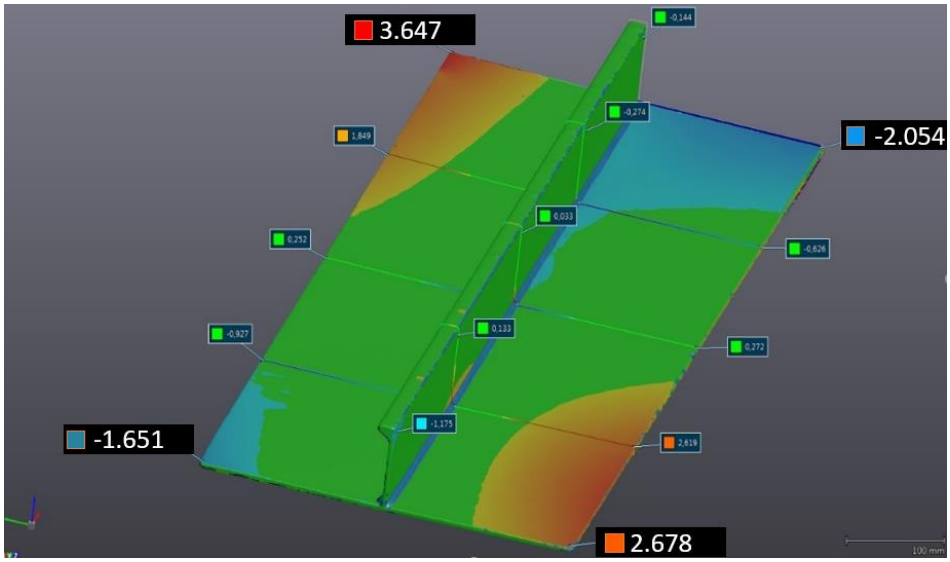

Figure 4.13. 3D laser scanning of fillet welds [2] units in [mm].

In Figure 4.13 the corners on one diagonal are lifted, while in the opposite diagonal, corners are pressed down, indicated by negative values. This shows a twisting deformation after the two weld passes and the release of tack welds. This is possibly caused by the fact that the two weld passes have been going in the opposite directions.

The vertical corner displacements for the long plate, obtained by the forward-coupled thermal-mechanical FE-simulations on the long plate have also been obtained. These results have been obtained using the ISSC method, and the displacement field is seen in Figure 4.14. The characteristic behaviour resulting from the ISSC method is seen, with locked corners in the normal direction to the base plate. Both sequences of releasing tack welds gave identical results, and thus only one of them is presented here.

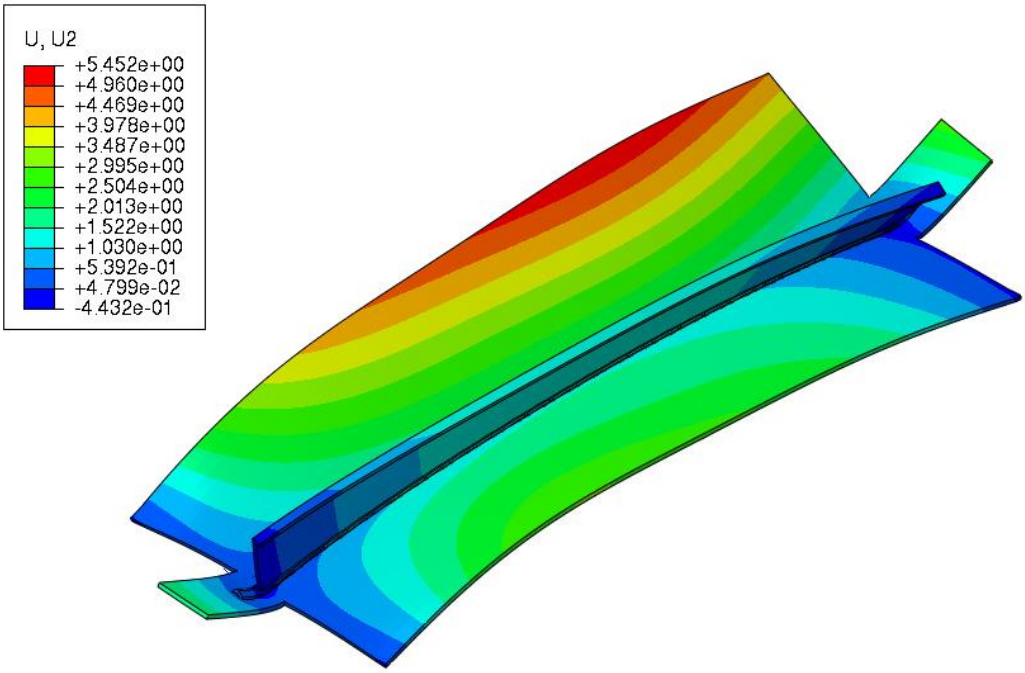

Figure 4.14. Deformation field [mm] on long plate, ISSC RBM method.

The resulting corner displacements for both the experimental results and the simulation results can be viewed in Table 4.4.

Table 4.4. Corner deformations [mm] on long plate, ISSC method.

Corner	Experiment	FE-simulation (contact)
A	3.647	4.51
B	-2.054	0
C	2.678	0
D	-1.651	0
Average displacement [mm]	0.655	1.128
		ISSC method

Since the ISSC method has been used, it is useful to look at the differences between the corners when comparing results, as is shown in Figure 4.15.

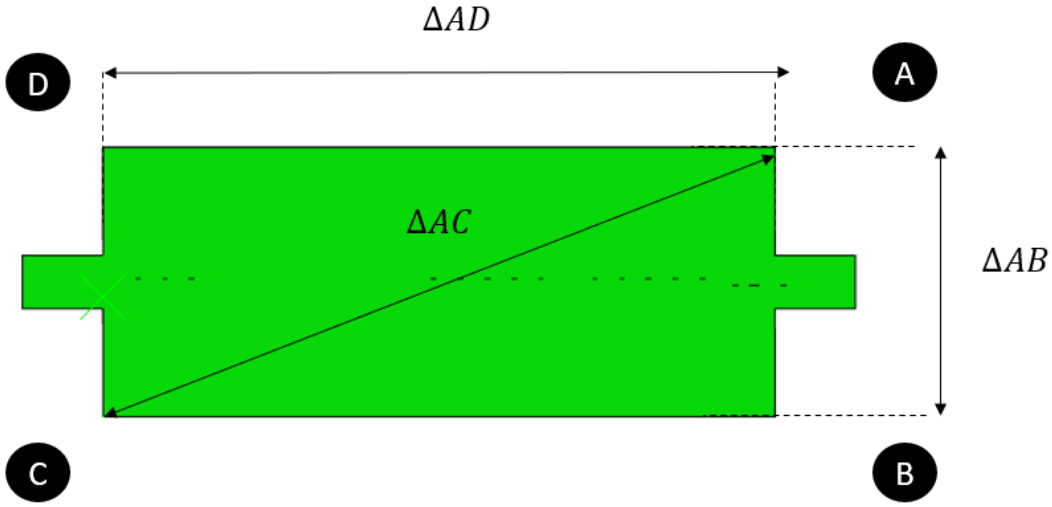

Figure 4.15. Scheme for comparing deformations.

For the experimental results, the difference between corner A and corner B becomes 5.7 mm, and between corner A and corner D the difference becomes 5.3. The diagonal difference for the experiment is from A to C and is 0.97 mm. For the FE-results the corresponding differences are $\Delta AD = \Delta AB = \Delta AC = 4.51$ mm.

4.2.4 Mechanical simulations and measured distortion angles

To further be able to validate the FE-model, the distortion angles from experiments seen in [3] can be compared to those obtained from simulations. The experiment conducted in [3] is on a 7 mm plate and stiffener, after a double fillet weld. In this experiment Flux-Cored Arc Welding (FCAW) has been used, instead of the GMAW studied in this project.

The experimental setup can be seen in [3] and consists of a stiffener that is welded onto a plate with two fillets. The base plate is fixed to the table at three locations on one side of the plate, but is free to move on the other side, where measuring gauges have been located at three locations. The measuring gauge in the middle of the plate gave the mean

angular distortion out of 5 test specimens as 2.39˚. The gauge at the front corner gave a mean angular distortion of 2.16˚, and the third gauge at the back corner gave 2.34˚. In Figure 4.15 this would be at the locations in between A and D, at A and at D respectively.

The angular distortions from simulation can be seen in Figure 4.16, in the same order as the positions located in the experiment in [3]. The angular distortions are tabulated in Table 4.5.

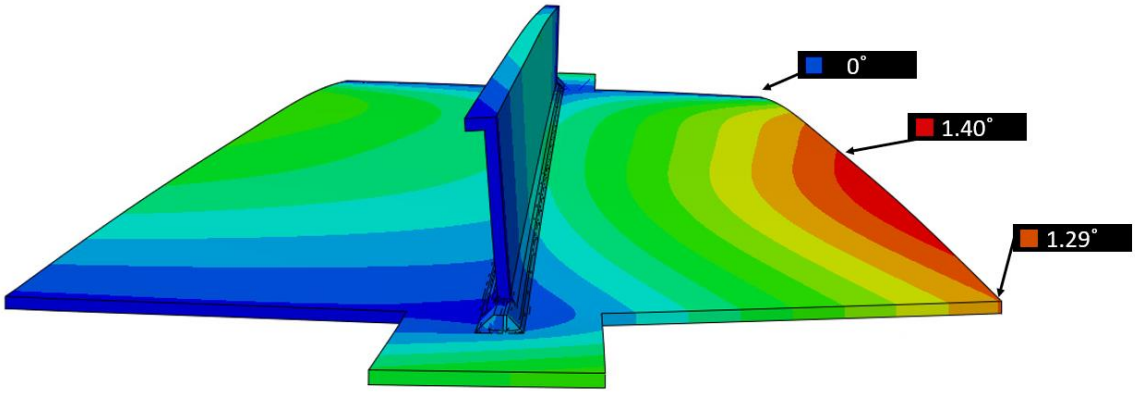

Figure 4.16. Angular distortions at locations 1 (1.29˚), 2 (1.40˚) and 3 (0˚).

Table 4.5: Angular distortions [3] compared to angular distortions obtained from FE-simulation.

Location		
1	2.16˚	1.29˚
2	2.39˚	1.4˚
3	2.34˚	0˚

4.2.5 Results from Group choice B and contact modelling

For the long plate three additional simulations were run, with a new method of preventing RBM as described in Figure 3.4. This method allows more movement and is a good proposal instead of the ISSC method. This method was used for two different sequences of releasing tack welds, but since the results were the identical regarding corner displacements, only one of these simulations will be presented. This method was also tested without contact modelling to see if the contact modelling is necessary, please see Table 4.6 for the results.

Table 4.6. Corner deformations on long plate [mm], Group choice B.

Corner	Experiment	FE-simulation (contact)	FE-simulation (no contact)
A	3.647	3.88	2.26
B	-2.054	0.15	0.41
C	2.678	3.777	-5.49
D	-1.651	0.297	0.23
Average displacement [mm]	0.655	2.026	-0.6475
		Group choice B	Group choice B

Similarly, as for the ISSC method it is interesting to look at the difference between vertical displacement at the corners, as visualised in Figure 4.15. These now become $\Delta AD = 1.85$ mm, $\Delta AB = 3.73$ mm and lastly $\Delta AC = 0.11$ mm. In Table 4.7 the differences are seen for the two methods tested with contact modelling, compared to the experiment.

Table 4.7. Comparison between vertical displacements [mm].

Vertical displacements			
ΔAD	4.51	1.85	4.3
ΔAB	4.51	3.73	5.7
ΔAC	4.51	0.11	0.97
	ISSC method	Group choice B	Experiment

For comparing the overall deformation, the deformation fields for the Group choice B method of preventing rigid body motion (b) is seen next to the ISSC method (a) in Figure 4.17. Here the colours represent the vertical displacement. To also see the effects of modelling contact, the deformation field for this plate is seen in 4.17 (c). Here it is seen that the table has a noticeable effect on the residual deformations.

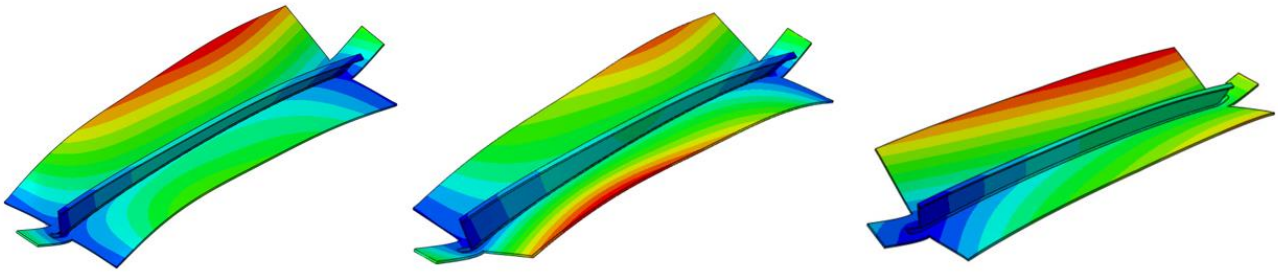

(a) ISSC **(b)** Group choice B (contact) **(c)** Group choice B (no contact)

Figure 4.17. Deformation fields on long plate.

5. Discussion

In this section a discussion on how to best model a moving heat source and two-pass fillet welding of a stiffener to a plate is presented. The assessments and recommendations are based on the forward-coupled thermal-mechanical FE-simulations on both the short and long plates, with comparison to both analytical and experimental results.

5.1 Cooling time and thermal simulations

The thermal simulations[3] on the short plate showed that a maximum temperature of 1000˚C with the actual weld speed characterized by a step time for the sequential heating of 4 s, gave reasonable cooling times with respect to analytical calculations [5]. Because of an uncertainty with the arc efficiency in the welding procedure, the welding speed could be altered to a small extent in the simulation procedure. When testing four additional speeds, it was found that a step time of 3 s gave a cooling time in the middle of the analytical range.

The cooling time between the two temperatures 800˚C and 500˚C is an important interval that describes the welding process with its given geometry and material [5]. These analytical calculations together with thermal simulations on the short plate proved to be an efficient way to both check the reasonability of the results from the FE-model, but also to further improve the modelling of a moving heat source from previous work seen in for example [6]. The results presented in Table 4.1 shows than a faster weld speed will lower the cooling time in this interval. Table 4.1 also shows that a higher temperature prescribed to the weld regions will increase the cooling time in this interval. These results are drawn based on the modelling of the moving heat source used in this project.

5.2 Tack release sequences and its effect on residual deformations

Four FE-simulations were run to study the effect of sequence when releasing the tack welds[4]. When studying the vertical corner displacement on the short plate, and how different sequences of releasing tack welds affected those, it was found that no specific release sequence affects the deformation. However, since the tack welds must be released, one sequence is necessary. Thus a counterclockwise sequence was deemed reasonable since this is physically possible for a welder to perform. That the sequence of releasing tack welds does not affect the residual deformations is reasonable since it is expected that the response to removal of fasteners after the welding process will be elastic in nature. The residual stresses and deformations in the plate have been caused by the two welding passes and are not affected by how the plate is handled after this process and once it has cooled down.

5.3 Rigid body motion and contact modelling

Five FE-simulations showed that one important aspect when modelling the release of the tack welds, that hold the plate to the table, is to prevent RBM as the plate now is free. If RBM is present, the results will not be reasonable, or convergence will not be accomplished in ABAQUS. In ABAQUS there are several methods of preventing this from happening, of which all affect the final results. The benchmark exercise that this

[3] Seven thermal FE-simulations have been run for this purpose with an average run time in the computer room of 20 minutes.

[4] The average time to run the thermal-mechanical simulations in the computer room was 94 minutes.

project is part of, recommends the ISSC method that was described in Figure 3.2, where in total 6 degrees of freedom are locked at a final simulation step. In addition to this method, three other procedures have been studied. The best way of preventing RBM is to do it in a way that prevents RBM and at the same time allows for an accurate representation of the real world within the models intended use.

The ISSC method does not seem to accurately represent the real world, since it prevents three corners from moving normal to the plate. Thus, the plate will be held down at these corners, even though the tack welds are removed. However, this method was chosen since it provides a general way of preventing RBM recommended by ISSC. In Figure 4.2, the vertical displacements are seen on the shorter plate when using this method.

However, since participants in the benchmark exercise are free to choose other methods to prevent RBM, this project has also studied inertia relief and one additional method on the short plate early on in the project. With inertia relief in ABAQUS, contact modelling cannot be used in the same model. When using inertia relief the result became unreasonable with large deformations, which may be because no table could be modelled in this attempt. Thus inertia relief for preventing RBM was not further investigated in this project.

A second choice of method called Group choice A was used early on in the project on the short plate. This method did not lock three corners in normal direction, as the ISSC method does. Thus the deformation of the plate will be more realistic in the sense that the plate can then deform more freely as it would in reality after releasing what is holding the plate down, as is seen in Figure 4.3. Here normal displacements are seen also at the corners that are locked using the ISSC method. For the long plate, the Group choice B method was also tested to see if this method could become more realistic. It showed that the overall shape of the deformed plate became closer to the experimental deformation field, however the vertical displacements did not fit the experimental data as well as for the ISSC method. The residual deformations were obtained for the long plate, with and without contact modelling activated, when using Group choice B. This showed that the contact modelling has an effect on the results and should therefore be included.

5.4 Residual stress state and comparison to experimental values on long plate

On the long plate (1000 mm), five simulations have been run on the PC-cluster Vera[5].When analysing the stresses, it was seen that the maximum values at the weld in both tension and compression were much greater than what should be expected from the material used in this project. The minimum yield point is 355 MPa and hardening is also included which allows for even higher stresses. However, in some areas the stress in each direction (longitudinal, transverse, and normal) was about 400 MPa higher than what would be expected from the material in this project. This is a result of the sequential heating, where all elements in a small region is heated simultaneously with the same prescribed temperature. The temperature only changes volume and not shape. This leads to locally too high hydrostatic stresses which does affect the von Mises effective stress

[5] The average time to run the thermal simulation for the long plate on the PC-cluster on 24 CPUs, was 100 minutes, and for thermal-mechanical simulation 620 minutes.

and yielding does not occur. The way of handling heat input thus enhances these hydrostatic stresses, which results in too high stresses at some point in all directions. Thus, these very high stresses were seen on the long plate, especially at the weld region. This can for example be seen in Figure 4.8 of the longitudinal residual stress inside of weld, by the grey areas. However, this phenomenon only occurs at certain points and thus the chosen way of modelling the moving heat source still provides a good, simplified approach.

When comparing the residual stresses obtained from simulations with experimental data at the base plate, the results from the simulations are seen to be reasonable. The longitudinal stresses both follow the same pattern with tension near the weld, and compression further out, and also have the same magnitudes. Here the hydrostatic stresses do not seem to affect these results, and they are mostly present on certain points at the weld. The same can be said for the transverse and normal stress at the base plate.

Regarding the normal and transverse residual stresses, these also follow the same pattern as for the experimental data, with similar amplitudes. Thus, the experiments made on a similar plate, exposed to two weld passes shows that the FE-model gives results close to reality and that the modelling method can be further implemented on other geometries as well besides the benchmark geometry. However, since the experimental geometry has some differences to the benchmark geometry, this is not known to its full extent.

5.5 Measured deformation field compared to FE-simulations on long plate

The measured deformation field was presented along with the FE-results in Table 4.4. Here it was seen that the magnitudes of the displacements were in the same neighbourhood. When using the ISSC method of preventing RBM, it is useful to look at the difference in displacement between the corners. The experimental results gave roughly the same differences as from the FE-simulations. However, the general shape of the deformed panel is not the same for the two methods. The experiment shows a clear twisting deformation with pushed up corners on one diagonal and pressed down corners on the other diagonal. The FE-results on the long plate do not seem to capture this behaviour seen in reality. However, when the differences in vertical displacement between the corners are of interest, this twisting behaviour is not of interest when comparing. When testing an additional method of preventing RBM the overall deformation field became more similar to experimental results, however the vertical displacements did not match as well.

5.6 Measured angular distortion compared to FE-simulations on long plate

The measured angular distortions in [3] was in a range between $[2.16^{\circ}, 2.39^{\circ}]$, and the angular distortions obtained from the simulations on the long plate was in a range between $[0^{\circ}, 1.40^{\circ}]$. That the angular distortions are lower from the FE-simulations is probably a consequence of the ISSC method of preventing RBM. Since three out of four corners are locked in vertical direction, this will press the plate down preventing the free movement of the corners in vertical direction. It appears to be easier to predict the residual stresses than to predict the welding deformations.

6. Conclusion and recommendations to the ISSC benchmark

In this project the conclusions drawn can be presented in the form of recommendations to the ISSC benchmark exercise. In total four different recommendations have been determined, as a result of this project of studying deformations and stresses in welded panels. The recommendations are based on simulations of both the short and long plate, and also experimental results for similar processes.

- The maximum temperature when modelling a moving heat source, should be 1000˚C to get an optimal 800˚C to 500˚C cooling time for the simplified heat source modelled used. This should be combined with a step time of 3 s when dividing each weld pass into 5 regions for the short plate.
- The sequence of releasing the tack welds, holding the base plate to the table, does not affect the residual deformations in the long plate. However, one realistic sequence has to be chosen so that the tack welds can be removed. Alternatively, releasing the tack welds all at once can simplify the model by reducing simulation steps.
- For realistic results, mechanical contact between the table and the plate should be modelled. When using the ISSC method of preventing RBM, the vertical displacements at the corners are the same with and without the table modelled but the deformed shape is not fully captured.
- Modelling a moving heat source by dividing its path into several sections, and then prescribing all elements within this section with the same temperature, can be a good and simplified model for the heat input. However, the recommendation to ISSC benchmark exercise is to be careful when analysing the residual stress state since this method in combination with element type used in the weld metal, causes high local hydrostatic stresses that will not be recognised by ABAQUS to cause yielding.

7. Future Work

An interesting future investigation is to further study a method of how rigid body motion can be prevented after releasing tack welds. In both ISSC-method and Group choice A, the focus has been to constrain a total of 6 dof on the corners of the base plate. Therefore, it would be of interest to study a combination of locking degrees of freedom mainly on the stiffener. An example is to constrain the base plate where the stiffener is placed, i.e. constrain all translations on the base plate where the stiffeners are and constrain the opposite side in only vertical direction. This gives four constrained degrees of freedom. Also, a corner needs to be locked along and normal to the base plate. This in total gives that 6 dof are constrained. Using this kind of prevention of RBM in ABAQUS, will free the sides and probably result in a deformation of the base plate that is closer to reality after releasing of the tack welds.

When analysing the residual stresses of the long plate, it was found that at some points on the weld, hydrostatic stresses were present. Therefore, to prevent hydrostatic stresses affecting the results, the way of heat input can further be investigated. In this project, sequential heating has been used which is a valid way of modelling the moving heat source since the residual stresses were close to experimental data. To minimize or exclude the hydrostatic stresses, it can be advantageous to model the moving heat source as gradual heating of elements, i.e. applying a heat flux. By gradually heating up elements, this might lead to more realistic results, closer to those obtained from experiment, but also decrease the appearance of the hydrostatic stresses. Other element types, and/or a finer mesh in the longitudinal direction should also be explored.

Further, in this project the FE-simulations performed are using a forward-coupled thermal-mechanical FE-analysis to simulate the welding process with material and geometrical nonlinearity incorporated. This means that heat generated by deformation is not considered in the thermal simulations. Therefore, an additional investigation can be to consider this phenomenon and study to what extent it affects the results.

References

[1] B.L. Josefson, M. McDill and S. Gurram. *Deformations and stresses in welded panels. Presentation to TME131 Chalmers University of Technology*. Gothenburg, Feb. 23, 2021.

[2] B.L. Josefson. ISSC 2021 V.3. *Materials & Fabrication Technology. Outline of the modified welding deformation benchmark. Personal communication.* (25-03-2021).

[3] J. Kozak and J. Kowalski. (2015). *Problems of Determination of Welding Angular Distortion of T-Fillet Joints in Ship Hull Structures.* Polish Maritime Research 2(86), 79-85.

[4] B.L. Josefson. ISSC 2021 V.3. *Modelling Approach. Personal communication.* (25-03-2021).

[5] K. Easterling. (1992). *Introduction to the Physical Metallurgy of Welding.* 2nd ed. Oxford; Boston: Butterworth Heinemann, p. 24-25.

[6] B. Pamfil, D. Hård, S. Gurram and S. Selvaraj. *Deformations in welded panels.* Report 2020:02, Department of Mechanics and Maritime Sciences, Chalmers University of Technology, Göteborg, Sweden. Retrieved from https://hdl.handle.net/20.500.12380/301201 (2021-04-15).

[7] B.L. Josefson. *Personal communication.* (15-04-2021).

[8] ABAQUS Inc. (2021). *Inertia relief.* Retrieved from https://classes.engineering.wustl.edu/2009/spring/mase5513/abaqus/docs/v6.6/books/usb/default.htm?startat=pt04ch11s01at31.html. (2021-05-08).

[9] ABAQUS Inc. (2021). *Abaqus/Standard Element Index.* Retrieved from http://130.149.89.49:2080/v6.7/books/usb/default.htm?startat=pt10eli01.html (2021-04-15).

CHALMERS
UNIVERSITY OF TECHNOLOGY